European Journal of Pharmacology 784 (2016) 121–128

Contents lists available at ScienceDirect

European Journal of Pharmacology

journal homepage: www.elsevier.com/locate/ejphar

Molecular and cellular pharmacology

Loading of Gemcitabine on chitosan magnetic nanoparticles increases the anti-cancer efficacy of the drug

Maryam Parsian [a,*], Gozde Unsoy [a], Pelin Mutlu [b], Serap Yalcin [c], Aysen Tezcaner [a,d], Ufuk Gunduz [a,e,*]

[a] Department of Biotechnology, Middle East Technical University, Ankara, Turkey
[b] Central Laboratory, Molecular Biology and Biotechnology R&D Center, Middle East Technical University, Ankara, Turkey
[c] Department of Food Engineering, Ahi Evran University, Kırşehir, Turkey
[d] Department of Engineering Sciences, Middle East Technical University, Ankara, Turkey
[e] Department of Biological Sciences, Middle East Technical University, Ankara, Turkey

ARTICLE INFO

Article history:
Received 12 April 2016
Received in revised form
6 May 2016
Accepted 10 May 2016
Available online 12 May 2016

Keywords:
Chitosan
Magnetic nanoparticles
Gemcitabine
Targeted drug delivery
Breast cancer

ABSTRACT

Targeted delivery of anti-cancer drugs increase the efficacy, while decreasing adverse effects. Among various delivery systems, chitosan coated iron oxide nanoparticles (CsMNPs) gained attention with their biocompatibility, biodegradability, low toxicity and targetability under magnetic field. This study aimed to increase the cellular uptake and efficacy of Gemcitabine.

CsMNPs were synthesized by in situ co-precipitation and Gemcitabine was loaded onto the nanoparticles. Nanoparticle characterization was performed by TEM, FTIR, XPS, and zeta potential. Gemcitabine release and stability was analyzed. The cellular uptake was shown. Cytotoxicity of free-Gemcitabine and Gem-CsMNPs were examined on SKBR and MCF-7 breast cancer cells by XTT assay.

Gemcitabine loading was optimized as 30 μM by spectrophotometric analyses. Drug release was highest (65%) at pH 4.2, while it was 8% at pH 7.2. This is a desired release characteristic since pH of tumor-tissue and endosomes are acidic, while the blood-stream and healthy-tissues are neutral. Peaks reflecting the presence of Gemcitabine were observed in FTIR and XPS. At neutral pH, zeta potential increased after Gemcitabine loading. TEM images displayed, Gem-CsMNPs were 4 nm with uniform size-distribution and have spherical shape. The cellular uptake and targetability of CsMNPs was studied on MCF-7 breast cancer cell lines. IC_{50} value of Gem-CsMNPs was 1.4 fold and 2.6 fold lower than free-Gem on SKBR-3 and MCF-7 cell lines respectively, indicating the increased efficacy of Gemcitabine when loaded onto nanoparticles.

Targetability by magnetic field, stability, size distribution, cellular uptake and toxicity characteristics of CsMNPs in this study provides a useful targeted delivery system for Gemcitabine in cancer therapy.

1. Introduction

Breast cancer is a prevalent cancer for women in the vast majority of countries worldwide (Bray et al., 2013). Despite the advances in treatments, the overall survival rate has not been improved substantially (Jemal et al., 2010). Conventional chemotherapeutic agents are unspecifically distributed all over the body where they affect both cancerous and normal cells. This treatment results in excessive toxicities. There is a need to develop novel approaches for therapies based on targeting of cancer cells. Recent advances in nanotechnology have explored new targeting strategies for enhancing intra-tumoral drug concentrations while limiting the systemic toxicity and side effects (Maeda, 2001).

Antitumor activity of Gemcitabine (2′,2′-difluorodeoxycytidine), a nucleoside analogue, has been reported in a variety of human tumors, including breast cancer in both experimental and clinical studies (Reddy and Couvreur, 2008). Gemcitabine inhibits DNA synthesis by incorporating into DNA. With its incorporation, DNA polymerase cannot add nucleotides leading to the termination of chain elongation, and induces apoptosis (Toschi et al., 2005). However, Gemcitabine could cause major systemic toxicities and drug resistance, which also restricts its therapeutic efficacy (Dasanu, 2008). The plasma level of this drug can quickly drop below the effective threshold level due to the short biological half-life (8–17 min) and its clinical benefit becomes limited. Thus, much larger doses are required to reach the effective plasma concentrations, increasing the risk of side effects. In addition, Gemcitabine is

* Correspondence to: Middle East Technical University, Department of Biotechnology, Inonu Boulevard, Universities Square, No: 1, 06800 Ankara, Turkey.
E-mail addresses: smaryamparsian@gmail.com (M. Parsian), gozdeunsoy@hotmail.com (G. Unsoy), ufukg@metu.edu.tr (U. Gunduz).

http://dx.doi.org/10.1016/j.ejphar.2016.05.016
0014-2999/

hydrophilic and it could not pass the plasma membrane by passive transportation (Lilly and Company, 1997) Therefore, it must be transported into the cells by nucleoside transporters, such as the human Equilibrative Nucleoside Transporters (hENT) (Bildstein et al., 2010; Chitkara et al., 2013). Cancer patients with tumors conveying lower hENT1 expression, have a considerably lower survival rate following Gemcitabine therapy as compared to patients with tumors that has a higher hENT1 expression. Moreover, many patients fail to benefit from the treatment due to the lack of the receptor (Farrell et al., 2009).

Few studies in the literature have been carried out for the development of Gemcitabine delivery system using nanoparticles which could reduce its side effects, increase internalization of the drug without receptor mediation and prolong its retention time (Arya et al., 2011; Hosseinzadeh et al., 2012; Garg et al., 2012; Arias et al., 2011). Chitosan has gained considerable attention due to its biocompatibility, biodegradability, and non-toxicity. Chitosan based delivery systems are widely used for the controlled delivery of drugs, proteins, and peptides (Braz et al., 2011; Rodrigues et al., 2012; Yongmei and Yumin, 2003). Chitosan coated magnetic nanoparticles were previously synthesized and characterized by our group (Unsoy et al., 2012, 2014a, 2014b). These nanocarriers, containing a magnetite (Fe_3O_4, iron oxide) core, could be actively targeted to the tumor site by an externally applied magnetic field after loaded with anti-cancer drugs. This is the main advantage of MNPs. Another important utility of MNPs is their role in tumor visualization as MRI agents, which is also approved by Food and Drug Administration in clinical use (Gao et al., 2009; Wilczewska et al., 2012).

2. Material and methods

In this study, chitosan coated magnetic nanoparticles (CsMNPs) were loaded with Gemcitabine for tumor targeting. Characterization of the drug loaded nanoparticles was performed by Transmission electron microscopy (TEM), Fourier transform infrared spectroscopy (FTIR), X-ray photoelectron spectroscopy (XPS), and zeta potential analyses. Drug loading and release characteristics of the nanoparticles were investigated. The cellular uptake and targetability characteristics of CsMNPs were studied on MCF-7 breast cancer cell lines. The cytotoxicity of free Gemcitabine and Gemcitabine loaded CsMNPs on breast cancer cell lines was determined by XTT cell proliferation analysis.

Iron (II) chloride tetrahydride ($FeCl_24H_2O$), iron (III) chloride hexahydrate ($FeCl_36H_2O$) were obtained from Merck (Germany). Chitosan (LMW, degree of deacetylation (DD) $\geq$ 85%), Sodium tripolyphosphate (TPP), Ammonium hydroxide (NH_4OH), Phosphate buffered saline (PBS), RPMI-1640, Fetal Bovine Serum (FBS), Trypsin–EDTA, Gentamycin, were purchased from Sigma-Aldrich Chemie GmbH, (Germany). Gemcitabine hydrochloride was the product of Sigma-Aldrich (USA). Mechanical stirrer (Heidolf RZR 2021, Germany) was used in the nanoparticle synthesis. XTT cell proliferation assay kit (XTT) was supplied by Biological Industries, Israel Beit Haemek Ltd (Israel). XTT cell proliferation assay was measured at UV spectrophotometer 96 well plate reader (Multiskan GO, Thermo Scientific). Transmission Electron Microscopy, X-Ray Diffraction spectroscopy and Zeta-Potential measurements were carried in METU Central Laboratory.

2.1. In situ synthesis of chitosan coated magnetic iron oxide nanoparticles (CsMNPs)

Chitosan coated magnetic iron oxide nanoparticles were in situ synthesized by the precipitation of Fe(II) and Fe(III) salts in the presence of chitosan and TPP molecules according to Unsoy et al. (2012). Chitosan (0.15 g) was dissolved in 1% acetic acid, and the pH was adjusted to 4.8. Iron salts were dissolved in 0.5% chitosan solution. 10 ml of TPP and 25 ml of NH_4OH were added under the nitrogen (N_2) gas flow and at vigorous stirring (Mechanical stirrer, Heildolf RZR 2021, Germany). TPP was used for the cross linking of chitosan polymers. The resulting solution containing chitosan coated magnetic Fe_3O_4 nanoparticles were extensively washed with deionized water and separated by magnetic decantation for several times.

2.2. Gemcitabine loading on CsMNPs

CsMNPs (2.5 mg/ml) were mixed with different concentrations of Gemcitabine in methanol solution (100%) and rotated (Biosan Multi RS-60 Rotator) at 90 rpm with 5 s vibration intervals for 24 h inside the light protected tubes at room temperature. After the incubation period, Gemcitabine loaded CsMNPs were separated by magnetic decantation with a neodymium magnet for a few minutes and drug loading efficiency was quantified by measuring the amount of unloaded drug, remained in the supernatant with a UV spectrophotometer (Multiskan GO, Thermo Scientific) at 269 nm. (Eq. (1)). The absorbance of supernatant from drug unloaded CsMNPs was used as blank. Amount of Gemcitabine in supernatant was calculated with the help of standard curve. The standard curve was constructed with different concentrations of the drug (Gemcitabine concentration: 1.5–22.5 μg/ml, Absorbance 0.04–0.71 unit). The loading of Gemcitabine on CsMNPs was confirmed by FTIR, XPS and Zeta-potential (Malvern Nano ZS90) analyses. The FTIR, XPS and Zeta-potential analyses were carried out in METU Central Laboratory.

$$\text{Loading efficiency}(\%)=\frac{\text{Calculated drug concentration}}{\text{Theoretical drug concentration}}\times 100 \quad (1)$$

2.3. Release of Gemcitabine from CsMNPs

The release of loaded Gemcitabine from CsMNPs (2.5 mg/ml) was analyzed at three different pH values in acetate (pH 4.2, 5.2) and PBS (pH 7.2), buffers at 37 °C. The amount of released Gemcitabine was determined by measuring the absorbance of the supernatant spectrophotometrically at 269 nm in different time intervals.

2.4. Targeting of CsMNPs by magnetic field

The magnetic properties of CsMNPs was evaluated in a three well canal-connected slide (designed by Assist. Prof. Dr. Ender YILDIRIM, Department of Mechanical Engineering, Cankaya University). MCF-7 cells (2.10^4 cells/slide) were seeded. After incubation for 12 h medium is removed and the magnetic field is applied under the middle well of slide. The nanoparticle dispersed medium was injected to the canal in order to detect the accumulation of CsMNPs by magnetic field application of the nanoparticles after removal of magnetic field.

2.5. Cellular uptake of CsMNPs

CsMNPs were applied at a concentration of 2.5 mg/ml and incubated for 7 h at 37 °C. After the incubation, cellular uptake of CsMNPs were detected by Prussian blue staining method, including iron stain and pararosaniline solutions. To prepare iron stain solution, potassium ferrocyanide solution (Sigma-Aldrich) and hydrochloride acid (1:1 v/v) were mixed in a falcon tube. Pararosaniline solution was diluted with dH_2O (2%, v/v). The blue color is obtained by the reaction of ferrocyanide acid in iron stain

solution with CsMNPs. Pararosaniline solution stains MCF-7 cells to pink color. Nanoparticle treated and untreated MCF-7 cells were visualized under the microscopy (Fluorescence Microscope System DM6000, Leica).

2.6. Cytotoxicity of CsMNPs and Gemcitabine loaded CsMNPs

Cytotoxicity of CsMNPs and Gemcitabine loaded CsMNPs on MCF-7, SKBR-3 human breast cancer cell lines were determined by Cell Proliferation Assay with XTT Reagent (Biological Industries, Israel) according to manufacturer's instructions.

SKBR-3 and MCF-7 (6×10^3 cells/well) cells were seeded into the 96 well microtiter plates (Greiner) and incubated overnight at 37 °C in a 95% (v/v) humidified atmosphere with 5% (v/v) CO_2. Cells were exposed to Gemcitabine, CsMNPs, and Gemcitabine loaded CsMNPs, for 72 h. At the end of 72 h, XTT reagent was added and soluble product was measured at 496 nm by microplate reader (Multiscan GO, Thermo Scientific). Cells incubated in only cell culture media were used as control. Relative cell viability results for Gemcitabine, CsMNPs, and Gemcitabine loaded CsMNPs exposed cells are given. The cell viability in control groups was considered 100%.

3. Results

3.1. Gemcitabine loading onto CsMNPs

Gemcitabine loading was achieved as 16, 22, 30 μM with different initial drug concentrations 7.5, 15, 22.5 μg/ml, respectively (Fig. 1). The highest loading efficiency was obtained as 39% (30 μM) with the highest Gemcitabine concentration (22.5 μg/ml) and all the experiments continued with this preparation.

3.2. Release of Gemcitabine from nanoparticles

Gemcitabine release studies showed that CsMNPs have a pH dependent release pattern. Chitosan is soluble in diluted acids with a pH lower than pKa (about 6.3) (Mucha, 1997). At low pH, the free amino groups are protonated causing electrostatic repulsion between the polymer chains, enabling opening up the branches of the polymeric chains and thus release of entrapped drug (Szymańska and Winnicka, 2015). The release profiles of the drug from CsMNPs in acetate buffer at pH 4.2 and pH 5.2 are given in Fig. 2. The drug release was studied in the pH range of 4.2–5.2, due to the lysosomal and late endosomal pH is in the range of pH 3–5 (Lim et al., 2011). In this range of pH almost the entire drug load is released inside the cells. The release studies were continued up to

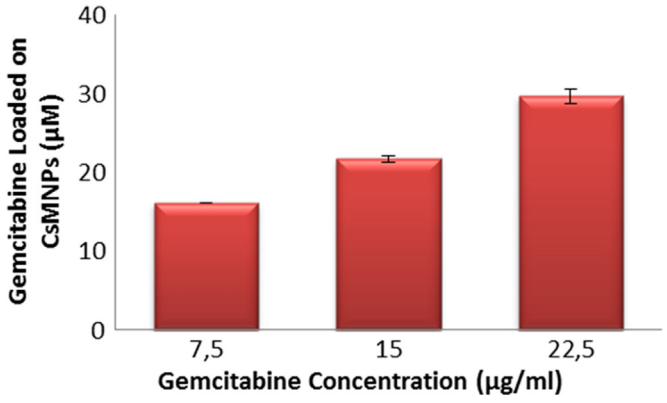

Fig. 1. Gemcitabine loaded on CsMNPs at different drug concentrations. The data are represented as the mean ± S.E.M. (n=3).

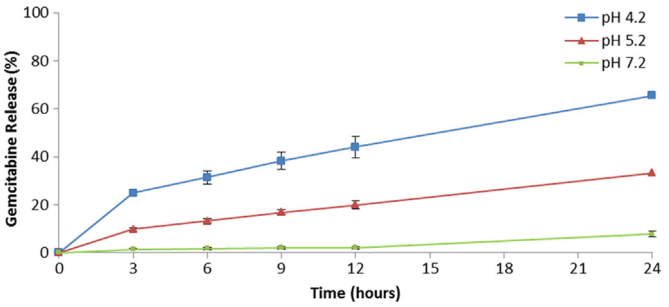

Fig. 2. Gemcitabine release profiles of CSMNPs in acetate buffer at pH 4.2, pH 5.2 and PBS buffer at pH 7.2. The data are represented as the mean ± S.E.M. (n =3).

24 h. Gemcitabine release was significantly higher at pH 4.2 (65.4%) compared to pH 5.2 (33%).

CsMNPs showed 25% and 10% initial burst release of Gemcitabine at pH 4.2 and 5.2, respectively during the first 3 h. This initial rapid release, characterized as "burst effect", occurs by desorption of Gemcitabine, localized on the surface of nanoparticles. Therefore, the rest of the drug must be entrapped into the mesh cavities of nanoparticles and released at a slower rate.

The release of Gemcitabine from the nanoparticles was also evaluated in PBS (pH 7.2) at 37 °C, which mimics the physiological conditions for 72 h. Fig. 2 shows only 24 h comparing the drug release rates of CsMNPs at different pH values. Results showed that the percentage of cumulative release was about 8%. During the first 12 h only 2% of the drug was released. Consequently, Gemcitabine loaded CSMNPs were highly stable at neutral pH.

3.3. Characterization of Gemcitabine loaded CsMNPs

3.3.1. Transmission electron microscopy (TEM) analyses

TEM images of CsMNPs and Gemcitabine loaded CsMNPs displayed almost spherical morphology and uniform size distribution (Fig. 3). The average diameters of CsMNPs were 4 nm and Gemcitabine loading did not significantly affect the sizes of the nanoparticles.

3.3.2. X-Ray photoelectron spectrophotometry (XPS) analyses

X-ray photoelectron spectrophotometry give insight to the interactions between the surface of chitosan coated iron oxide nanoparticles and Gemcitabine. XPS specifically reveals atomic composition of the nanoparticle's surfaces. Nitrogen and oxygen amounts did not change significantly upon loading of Gemcitabine which may be due to the fact that most of the loaded Gemcitabine enters into the cavities of chitosan network rather than attaching to the surface of nanoparticles (data not shown). However, the peak belonging to Fluorine atom of Gemcitabine appeared in the particular Fluorine analyses of drug loaded CsMNPs (between 670 and 700 eV binding energy and under 1200 c/s), demonstrating the presence of Gemcitabine on the surface of CsMNPs.

3.3.3. Fourier Transform-Infrared Spectroscopy (FTIR)

The CsMNPs and Gemcitabine loaded CsMNPs were characterized by the FTIR. In FTIR spectra of drug loaded nanoparticles the bands coming from both the CsMNPs and from free Gemcitabine were observed (Fig. 4). FTIR spectra of Gemcitabine revealed high intensity broad bands at approximately 2932, 1689, and 1055 cm^{-1}. These peaks were also observed in the spectrum of Gemcitabine loaded CsMNPs as shifted to 2920, 2850 cm^{-1} (CH2), 1689 cm^{-1} (C=O) and 1053 cm^{-1} (C–O). However, these peaks were not present in the spectrum of CsMNPs. This is a clear indication of Gemcitabine loading on chitosan coated magnetic nanoparticles.

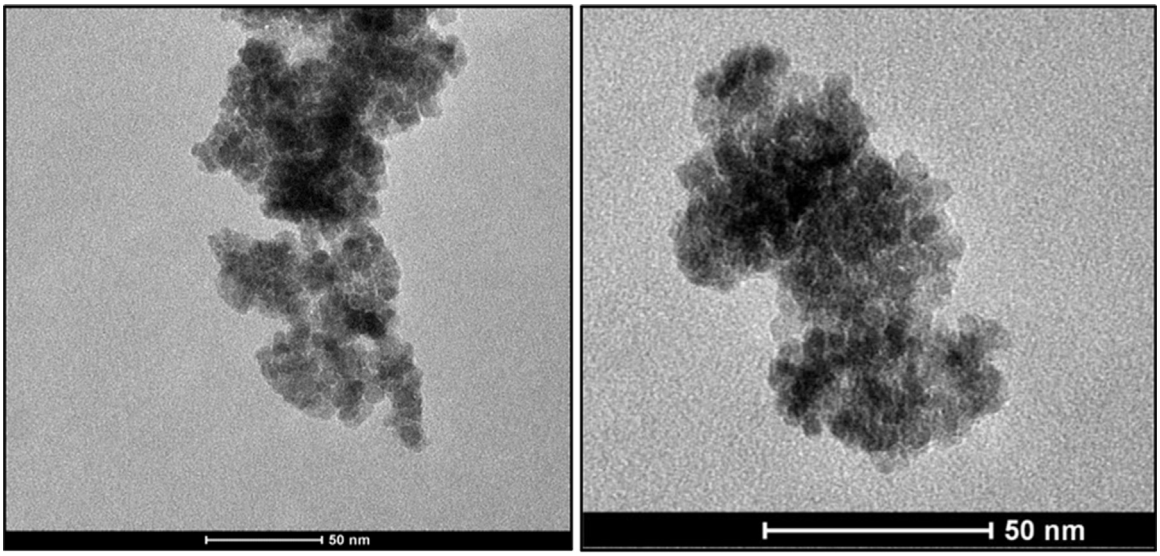

Fig. 3. TEM images of CsMNPs (a) and Gemcitabine loaded CsMNPs (b).

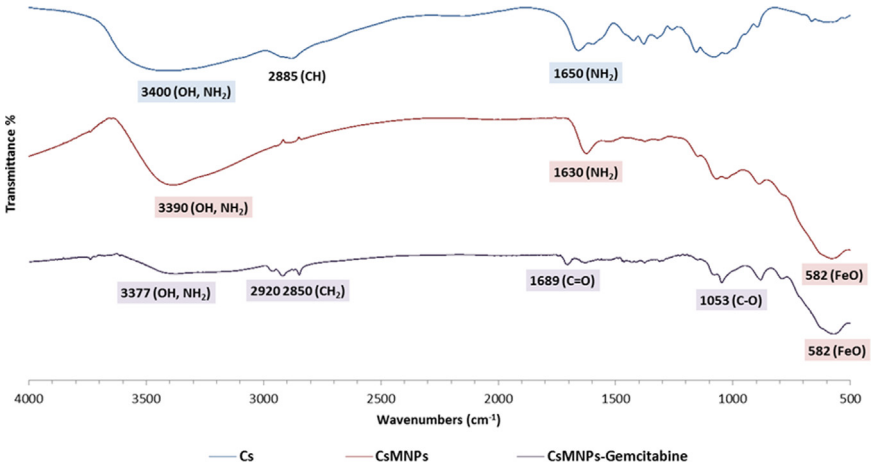

Fig. 4. FTIR spectra of CsMNPs and Gemcitabine loaded CsMNPs.

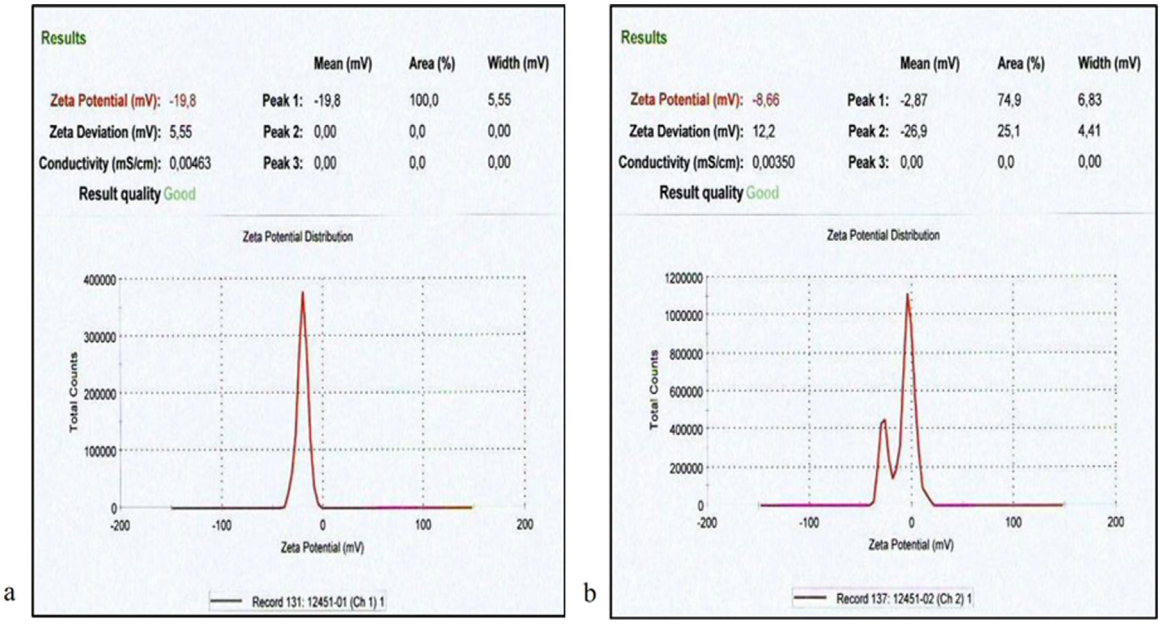

Fig. 5. Zeta potential measurements of CsMNPs (a) and Gemcitabine loaded CsMNPs (b). The number of runs is triplicate.

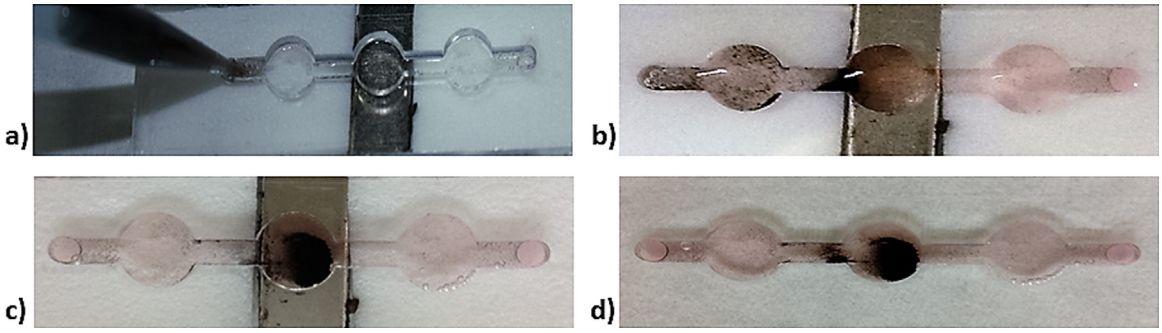

Fig. 6. Targeting of CsMNPs; injection of CsMNPs to the canal (a) and accumulation of CsMNPs (b, c) by magnetic field. Dispersion of the nanoparticles after the removal of magnetic field (d).

3.3.4. Zeta (ζ) potential analysis

The zeta potential of CsMNPs was determined as −20 mV in aqueous medium at pH 7.2. Unsoy et al. (2012) reported that CsMNPs have negative charge at pH > 6.7 due to the deprotonation of amino groups on chitosan layer. An electrostatic interaction is expected between the aqueous dispersion of negatively charged CsMNPs (pH 7.2) and positively charged Gemcitabine (by the protonation of NH2 group). Zeta potential of Gemcitabine loaded CsMNPs was −9 mV at pH 7.2. This significant increase in zeta potential from −20 mV to −9 mV could be explained by entrapment of Gemcitabine to the chitosan coated iron oxide nanoparticles and neutralizing the negative charge (Fig. 5).

3.3.5. Targeting of CsMNPs by magnetic field

The targeting of chitosan magnetic nanoparticles were investigated in a MCF-7 cells seeded slide. The targetability of CsMNPs are shown in Fig. 6. After the magnetic field application, all of the CsMNPs were accumulated in the middle well, that the magnetic field is applied. None of the nanoparticles have passed to the third well. When the slide was removed away from the magnetic field, CsMNPs have dispersed in the medium again. The light microscope images of middle wells of cell seeded slides is given in Fig. 7.

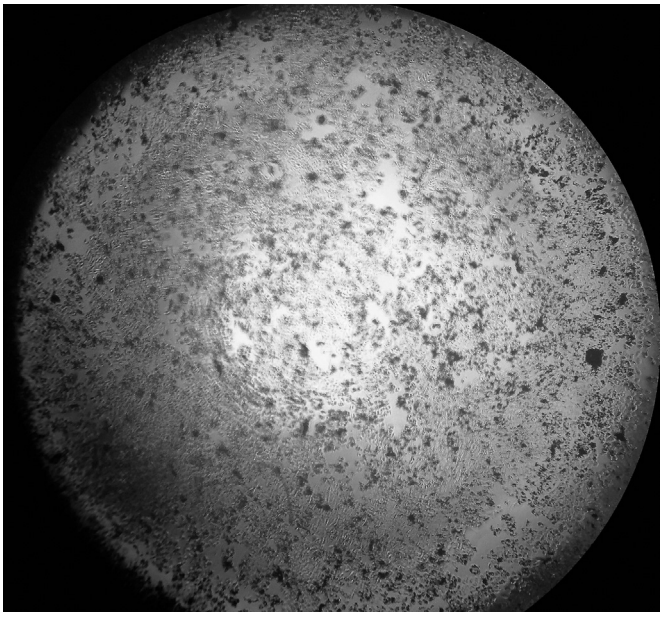

Fig. 7. Light microscopy image of CsMNPs applied MCF-7 cells seeded in the middle well of the slide.

3.3.6. Cellular uptake of CsMNPs

The nanoparticles dispersed in the medium were given to the MCF-7 cells for 7 h (Fig. 8). The blue colored CsMNPs were taken up by the cells and color of the cells, which internalize nanoparticles, get darker than the control cells. The color of nuclear membrane appeared significantly darker than in the control cells. This implies the accumulation of CsMNPs around the nucleus during this incubation time. Even the agglomerates formed after the staining of CsMNPs were observed as adhered on the cells though the harsh washing steps of MCF-7 cells.

3.3.7. Cytotoxicity of CsMNPs and Gemcitabine CsMNPs on SKBR-3 and MCF-7 cells

XTT results showed that unloaded CsMNPs were not significantly cytotoxic on SKBR-3 cells up to 1.7 mg/ml concentration. On the other hand, 0.8 mg/ml CsMNPs caused 30% cell death on MCF-7 cells (Fig. 9). However, much lower amounts (less than 0.5 mg/ml) of CsMNPs were used for drug loading studies which is not significantly cytotoxic.

Fig. 10 demonstrates the dose dependent anti-proliferative effect of free Gemcitabine and Gemcitabine loaded CsMNPs on MCF-7 and SKBR-3 cell lines. IC_{50} values of Gemcitabine and Gemcitabine loaded CsMNPs were 3.6 μM and 1.5 μM on MCF-7 cells and 6.5 μM and 4.8 μM on SKBR-3 cells, respectively (Fig. 10). Results showed that, Gemcitabine loaded CsMNPs were found as nearly 2.6 and 1.4 fold more toxic compared to free Gemcitabine on MCF-7 and SKBR-3 cells, respectively. These results showed that Gemcitabine loaded on CsMNPs are more effective on both breast cancer cell lines.

4. Discussion

Easy synthesis, chemical stability in physiological conditions, possibility of coating by polymeric shells and loading with various agents make iron oxide (Fe_3O_4, magnetite) nanoparticles favorable for biomedical use (Sun et al., 2008; Nune et al., 2009). Chitosan coated magnetic nanoparticles (CsMNPs) were synthesized for targeting drugs to the tumor cells in the presence of magnetic field. By this way the drug concentration may be increased in a specific target tissue compared with the rest of the body. The targeting and accumulation of CsMNPs via magnetic field application was shown in this study (Figs. 6 and 7). In our previous studies, the magnetic core of CsMNPs was found as superparamagnetic by Vibrating sample magnetometry (VSM) analyses (Unsoy et al., 2012). Superparamagnetic nanoparticles show magnetic properties just in the presence of magnetic field, which is a desired characteristic in biomedical applications (Unsoy et al., 2012; Khodadust et al., 2013). Chitosan coat on the surface of magnetic nanoparticles reduces the agglomeration, and provides internal cavities for loading of therapeutics and adding functional

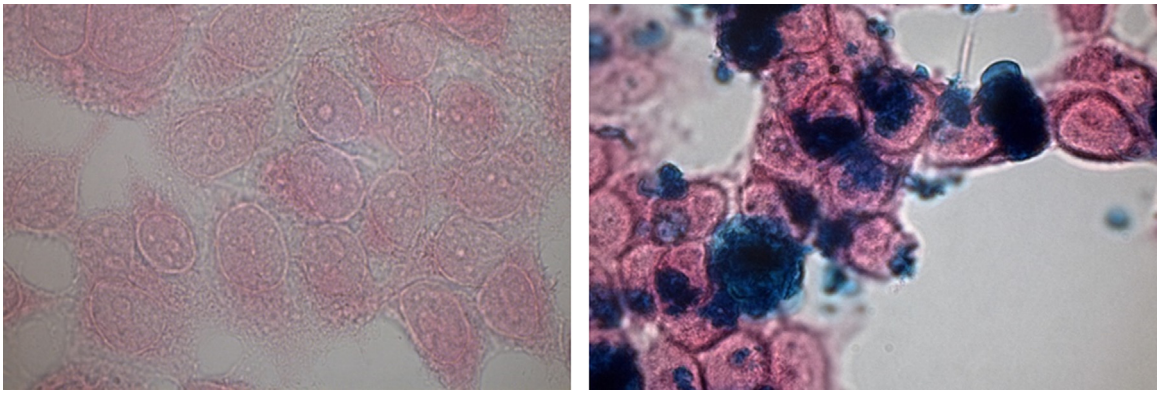

Fig. 8. The bright field microscope images of untreated control (left) and Prussian Blue stained CsMNPs treated (right) MCF-7 cells. (For interpretation of the references to color in this figure legend, the reader is referred to the web version of this article.)

groups (Unsoy et al., 2014a, 2014b; Andrade et al., 2011). In this study, an anti-cancer drug, Gemcitabine was loaded onto CsMNPs, which was verified by UV spectophotometric measurements, XPS, Zeta-potential, and FTIR.

The results of TEM analysis displayed nanoparticles with uniform size distribution of 4 nm on the average. Particle size observed by TEM reflects only the magnetite (Fe_3O_4) core of the nanoparticles, because the loose chitosan layer collapses during the drying process before TEM analysis. Previous studies in our laboratory with dynamic light scattering (DLS) nanosizer indicated that the hydrodynamic diameters of CsMNPs were about 60 nm (Unsoy et al., 2012). In the case of intravenous administration, nanoparticles larger than 200 nm diameter can activate human complement systems and be phagocytized by Kupffer cells (Aggarwal et al., 2009). Kulkarni and Feng (2011) validated that their small sized (<200 nm) nanoparticles can escape from recognition by the reticuloendothelial system (RES) and prolong the half-life of the nanoparticles in the blood circulation. Longer blood circulation time increases the availability of the nanoparticles in the body. The size of the nanoparticles plays a key role in their adhesion to and interaction with the cells. Nanoparticles with sizes smaller than 200 nm are efficiently taken up by the cancer cells via endocytosis in vitro (Foster et al., 2001). Therefore, our CsMNPs are expected to escape from reticuloendothelial system (RES) and be taken up by tumor cells. In the literature, there are few studies related to Gemcitabine loaded chitosan nanoparticles, however most of them do not contain magnetite (Arya et al., 2011). Among these nanoparticles, the size range is between 80 and 400 nm (Hosseinzadeh et al., 2012; Garg et al., 2012; Arias et al., 2011). When low molecular weight chitosan was used with low amounts of TPP in the synthesis; a smaller sized, more porous and loose structured nanoparticles, with many cavities for drug entrapment, were obtained (Hosseinzadeh et al., 2012; Unsoy et al., 2012). This is advantageous for targeted drug delivery effecting the loading and release characteristics of CsMNPs.

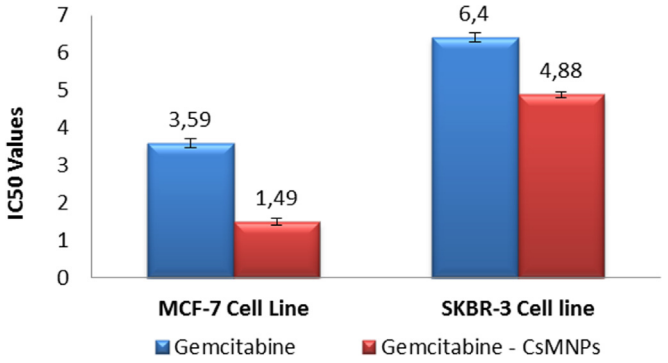

Fig. 10. IC_{50} values of free Gemcitabine and Gemcitabine loaded CsMNPs in MCF-7 and SKBR-3 cell lines.

Zeta potential of CsMNPs was determined as negative around

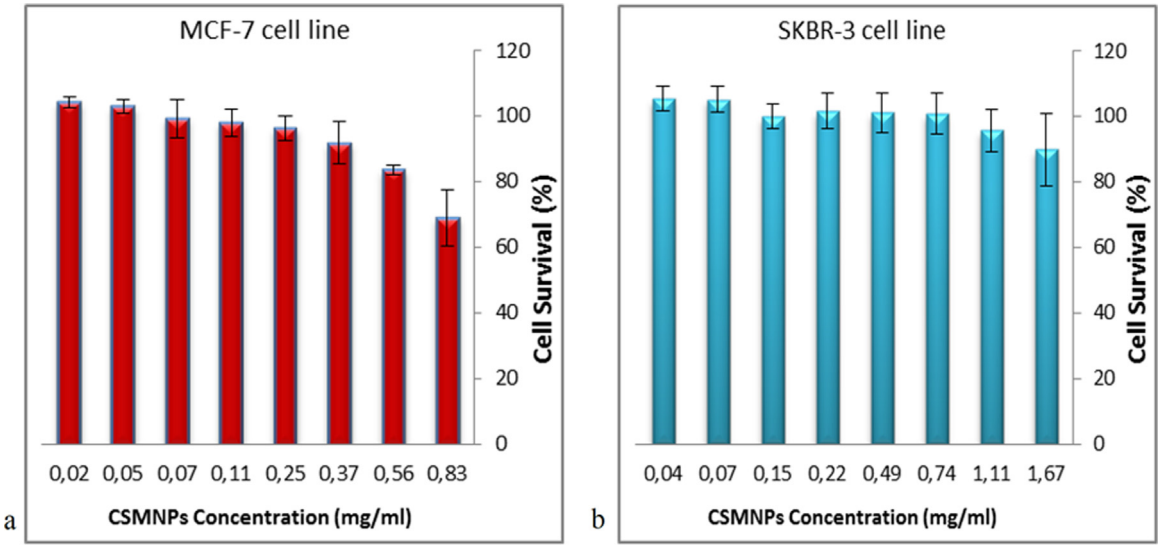

Fig. 9. Cytotoxicity of CsMNPs on MCF-7 (a) and SKBR-3 (b) cell lines. The data are represented as the mean ± S.E.M. (n=2).

the neutral pH (Unsoy et al., 2012). The zeta potential shifted towards more positive direction after loading with Gemcitabine (Fig. 5). This may be due to positive charge of Gemcitabine which probably masks the surface charge of CsMNPs. The negative domains of cell membrane can interact with Gemcitabine loaded CsMNPs by nonspecific electrostatic interactions to facilitate their cellular uptake. In addition to surface charge, it was found that the cellular uptake was heavily dependent on size. In this study, CsMNPs were successfully taken up by MCF-7 cells. The efficient cellular internalization of CsMNPs were previously demonstrated on various cell lines by our group (Unsoy et al., 2012). Huang et al. (2002) was also reported that A549 cells internalize chitosan nanoparticles predominantly by clathrin-mediated adsorptive endocytosis, not by fluid endocytosis or passive diffusion. Cellular internalization of N-acetyl histidine-conjugated glycol chitosan nanoparticles was also occurred by adsorptive endocytosis (Park et al., 2006).

The drug release was measured in acetate buffer at two different pH values (pH 4.2 and pH 5.2) up to 24 h. Higher release of Gemcitabine was obtained at pH 4.2 (65%) which is probably due to the decomposition of chitosan at this pH (Braz et al., 2011). Gemcitabine release from CsMNPs indicated a pH dependent release pattern. As the pH of the medium was decreased, the drug release increased. Therefore, Gemcitabine is expected to be released inside the cancer cells, because the pH of tumor tissue and endosomes are acidic (pH 3–5) (Lim et al., 2011; Park et al., 2006; Decuzzi et al., 2007; Sahu et al., 2010). The burst release of 25%, 10% Gemcitabine at pH 4.2, 5.2, respectively, indicated that low amount of drug was associated with the surface and most of the drug was entrapped into the mesh cavities of CsMNPs. In the proof of XPS analysis, only small percentage of the drug was attached to the surface of CsMNPs because there was not a significant change on nitrogen and oxygen atoms upon Gemcitabine loading on the surface of nanoparticles.

Garg et al. (2012) investigated in vitro release kinetics of Gemcitabine from chitosan/poly(ethylene glycol)anisamide nanoparticles by dialysis bag method using PBS (10 mM, pH 5.8) as release medium. They showed that nearly 79% of the drug was released from CsMNPs during 10 days. In their case, Gemcitabine release from the nanoparticles was so slow due to the encapsulation of drug during the synthesis of high molecular weight polymeric structure. The presence of PEG together with chitosan seems to affect and slows down the release of the drug from the nanoparticles. Contrarily, Arias et al. (2011) obtained much faster Gemcitabine release rate from chitosan nanoparticles at pH 5. They observed 65% release within 2 h, while the remaining drug was slowly released in the next 22 h. This fast release was attributed to the high solubility of chitosan at pH 5. In our study, TPP cross-linker was used to prevent the rapid degradation of chitosan at pH 5.2. Therefore, CsMNPs released 33% of the loaded Gemcitabine at pH 5.2 in 24 h (Fig. 2) after the burst release (10%), which seems to be a reasonable release rate when compared to the previous studies in the literature. The release reflects that higher amounts of the drug were present in the internal cavities of the CsMNPs.

Arias et al. (2011) also reported that at pH 7.4, the entrapped drug within the nanoparticles showed burst release in the first 2 h (40%). This burst release is explained as the leakage of the surface associated drug, which rapidly diffused to the medium. The remaining drug was released throughout the next 4 days. In our study, Gemcitabine release from CsMNPs was quite low (8%) in PBS buffer (pH 7.2, 37 °C) up to 72 h, which is advantageous for the stability of the drug in blood circulation. Actually, it is known that the half-life of free Gemcitabine is too short (8–17 min) at physiological conditions (Dasanu, 2008). On the other hand, 92% of the loaded Gemcitabine on CsMNPs retains up to 72 h at pH 7.2, which is a great improvement.

The burst release from CsMNPs in this study is $\leq 2\%$ at pH 7.2. In the study of Celia et al., the burst release of Gemcitabine from chitosan nanoparticles were 40% in the first 2 h studied at pH 7.4 (Celia et al., 2011).

As previously reported by Unsoy et al. (2014a) the efficacy of Doxorubicin loaded CsMNPs was 2 folds higher than free Doxorubicin on MCF-7 cells. In another study we have carried out with Bortezomib loaded CsMNPs revealed that the IC_{50} decreases 2 folds as compared to free Bortezomib applied onto HeLa cells (Unsoy et al., 2014b). Findings of Vandana and Sahoo, also confirms these results in pancreatic cancer cells (Vandana and Sahoo, 2010). They have reported that IC_{50} of PEGylated Gemcitabine was 1.8 fold lower than free Gemcitabine. Consequently, higher degree of cell killing was achieved with the same drug concentrations when delivered by nanoparticles in vitro.

In this study, unloaded CsMNPs showed no cytotoxic effect on SKBR-3 and MCF-7 cells up to 0.5 mg/ml. Gemcitabine loaded CSMNPs were 1.4–2.6 fold more effective in killing of these two breast cancer cell lines as compared to free Gemcitabine. CsMNPs could increase the cellular uptake of Gemcitabine by endocytosis. Free Gemcitabine chloride could not pass through the plasma membrane easily due to its hydrophilicity.

The development of drug resistance is an important clinical complication, and the construction of drug loaded nanoparticles offer an opportunity to overcome this problem (Arias et al., 2011; Gao et al., 2009). Gemcitabine resistance caused by the loss of certain nucleoside transporters (hENTs) could be bypassed via nanoparticles since hENTs are not needed for internalization of the drug (Farrell et al., 2009). Cellular internalization of drug loaded nanoparticles occur through endocytosis. In the light of these results, Gemcitabine loaded CsMNPs may be a promising tool for breast cancer therapy.

5. Conclusion

Targeted drug delivery prevents adverse off-target effects, drug toxicities, and unnecessary systemic immunosuppression, while providing increased therapeutic efficacy. Moreover, tissue specific delivery may also increase the benefit of some drugs whose their use have been eliminated due to low bioavailability in affected tissues or prohibitively high toxicities in the rest of the body. Therefore, targeted drug delivery may solve many concerns.

In this study, synthesized chitosan magnetic nanoparticles are non-toxic, targetable by a magnetic field and quite stable in physiological conditions. Besides, Gemcitabine loaded chitosan magnetic nanoparticles exhibited higher anti-proliferative activity than free drug in vitro with pH dependent drug release characteristics. Consequently, Gemcitabine loaded CsMNPs may be a good targeted drug delivery system for clinical applications. Further in vivo studies are needed.

Conflict of interest

The authors of this study declare that they have no conflict of interest.

References

Aggarwal, P., Hall, J.B., McLeland, C.B., Dobrovolskaia, M.A., McNeil, S.E., 2009. Nanoparticle interaction with plasma proteins as it relates to particle biodistribution, biocompatibility and therapeutic efficacy. Adv. Drug Deliv. Rev. 61 (6), 428–437.

Andrade, F., Antunes, F., Nascimento, A.V., Baptista da Silva, S., das Neves, J., Ferreira, D., Sarmento, B., 2011. Chitosan formulations as carriers for therapeutic proteins. Curr. Drug Discov. 8, 157–172.
Arias, J.L., Reddy, L.H., Couvreur, P., 2011. Superior preclinical efficacy of gemcitabine developed as chitosan nanoparticulate system. Biomacromolecules 12, 97–104.
Arya, G., Vandana, M., Acharya, S., Sahoo, S.K., 2011. Enhanced antiproliferative activity of Herceptin (HER2)-conjugated gemcitabine-loaded chitosan nanoparticle in pancreatic cancer therapy. Nanomed.: Nanotechnol. Biol. Med. 7 (6), 859–870.
Bildstein, L., Dubernet, C., Marsaud, V., Chacun, H., Nicolas, V., Gueutin, C., Sarasin, A., Bénech, H., Lepêtre-Mouelhi, S., Desmaële, D., Couvreur, P., 2010. Transmembrane diffusion of gemcitabine by a nanoparticulatesqualenoyl prodrug: an original drug delivery pathway. J. Control Release 147, 163–170.
Bray, F., Ren, J.S., Masuyer, E., Ferlay, J., 2013. Global estimates of cancer prevalence for 27 sites in the adult population in 2008. Int. J. Cancer 132, 1133–1145.
Braz, L., Rodrigues, S., Fonte, P., Grenha, A., Sarmento, B., 2011. Mechanisms of chemical and enzymatic chitosan biodegradability and its application on drug delivery. In: Felton, G. (Ed.), In Biodegradable Polymers: Processing, Degradation and Applications. Nova Science Publisher, New York, NY, USA.
Celia, C., Cosco, D., Paolino, D., Fresta, M., 2011. Gemcitabine-loaded innovative nanocarriers vs GEMZAR: Biodistribution, pharmacokinetic features and in vivo antitumor activity. Expert Opin. Drug Deliv. 8 (12), 1609–1629.
Chitkara, D., Mittal, A., Behrman, S.W., Kumar, N., Mahato, R.I., 2013. Self-assembling, amphiphilic polymer-gemcitabine conjugate shows enhanced antitumor efficacy against human pancreatic adenocarcinoma. Bioconjug. Chem. 24, 1161–1173.
Dasanu, C.A., 2008. Gemcitabine: vascular toxicity and prothrombotic potential. Expert Opin. Drug Saf. 7, 703–716.
Decuzzi, P., Ferrari, M., 2007. The role of specific and non-specific interactions in receptor-mediated endocytosis of nanoparticles. Biomaterials 28, 2915–2922.
Lilly, Eli, Company, 1997. Summary of Product Characteristics: Gemcitabine UK Prescribing Information. Eli Lilly and Company, Indianapolis, Ind, USA.
Farrell, J.J., Elsaleh, H., Garcia, M., Lai, R., Ammar, A., Regine, W.F., Abrams, R., Benson, A.B., Macdonald, J., Cass, C.E., Dicker, A.P., Mackey, J.R., 2009. Human equilibrative nucleoside transporter 1 levels predict response to gemcitabine in patients with pancreatic cancer. Gastroenterology 136, 187–195.
Foster, K.A., Yazdanian, M., Audus, K.L., 2001. Microparticulate uptake mechanisms of in-vitro cell culture models of the respiratory epithelium. J. Pharm. Pharmacol. 53 (1), 57–66.
Gao, J., Gu, H., Xu, B., 2009. Multifunctional magnetic nanoparticles: design, synthesis, and biomedical applications. Acc. Chem. Res. 42 (8), 1097–1107.
Garg, N.K., Dwivedi, P., Campbell, C., Tyagi, R.K., 2012. Site specific/targeted delivery of gemcitabine through anisamide anchored chitosan/poly ethylene glycol nanoparticles: an improved understanding of lung cancer therapeutic intervention. Eur. J. Pharm. Sci. 47 (5), 1006–1014.
Hosseinzadeh, H., Atyabi, F., Dinarvand, R., Ostad, S.N., 2012. Chitosan–pluronic nanoparticles as oral delivery of anticancer gemcitabine: preparation and in vitro study. Int. J. Nanomed. 7, 1851.
Huang, M., Ma, Z., Khor, E., Lim, L.Y., 2002. Uptake of FITC-chitosan nanoparticles by A549 cells. Pharm. Res. 19 (10), 1488–1494.
Jemal, A., Siegel, R., Xu, J., Ward, E., 2010. Cancer statistics, (2010). Cancer J. Clin. 60, 277–300.
Khodadust, R., Unsoy, G., Yalcın, S., Gunduz, G., Gunduz, U., 2013. PAMAM dendrimer-coated iron oxide nanoparticles: synthesis and characterization of different generations. J. Nanopart. Res. 15 (3), 1–13.
Kulkarni, S.A., Feng, S.S., 2011. Effects of surface modification on delivery efficiency of biodegradable nanoparticles across the blood-brain barrier. Nanomedicine 6 (2), 377–394.
Lim, E.K., Huh, Y.M., Yang, J., Lee, K., Suh, J.S., Haam, S., 2011. pH-triggered drug-releasing magnetic nanoparticles for cancer therapy guided by molecular imaging by MRI. Adv. Mater. 23, 2436–2442.
Maeda, H., 2001. The enhanced permeability and retention (EPR) effect in tumor vasculature: the key role of tumor-selective macromolecular drug targeting. Adv. Enzym. Regul. 41, 189–207.
Mucha, M., 1997. Rheological characteristics of semi-dilute chitosan solutions. Macromol. Chem. Phys. 198 (2), 471–484.
Nune, S.K., Gunda, P., Thallapally, P.K., Lin, Y.Y., Laird Forrest, M., Berkland, C.J., 2009. Nanoparticles for biomedical imaging. Expert Opin. Drug Deliv. 6 (11), 1175–1194.
Park, J.S., Han, T.H., Lee, K.Y., Han, S.S., Hwang, J.J., Moon, D.H., Kim, S.Y., Cho, Y.W., 2006. N-acetyl histidine-conjugated glycol chitosan self-assembled nanoparticles for intracytoplasmic delivery of drugs: endocytosis, exocytosis and drug release. J. Control. Release 115, 37–45.
Reddy, L.H., Couvreur, P., 2008. Novel approaches to deliver gemcitabine to cancers. Curr. Pharm. Des. 14, 1124–1137.
Rodrigues, S., Dionísio, M., López, C.R., Grenha, A., 2012. Biocompatibility of Chitosan Carriers with Application in Drug Delivery. J. Funct. Biomater. 3, 615–641.
Sahu, S.K., Mallick, S.K., Santra, S., Maiti, T.K., Ghosh, S.K., Pramatik, P., 2010. In vitro evaluation of folic acid modified carboxymethyl chitosan nanoparticles loaded with doxorubicin for targeted delivery. J. Mater. Sci. – Mater. Med. 21, 1587–1597.
Sun, C., Lee, J.S., Zhang, M., 2008. Magnetic nanoparticles in MR imaging and drug delivery. Adv. Drug. Deliv. Rev. 60 (11), 1252–1265.
Szymańska, E., Winnicka, K., 2015. Stability of Chitosan—a challenge for pharmaceutical and biomedical applications. Mar. Drugs 13 (4), 1819–1846.
Toschi, L., Finocchiaro, G., Bartolini, S., Gioia, V., Cappuzzo, F., 2005. Role of gemcitabine in cancer therapy. Future Oncol. 1, 7–17.
Unsoy, G., Yalcin, S., Khodadust, R., Gunduz, G., Gunduz, U., 2012. Synthesis optimization and characterization of chitosan-coated iron oxide nanoparticles produced for biomedical applications. J. Nanopart Res. 14, 964–977.
Unsoy, G., Khodadust, R., Yalcin, S., Mutlu, P., Gunduz, U., 2014a. Synthesis of doxorubicin loaded magnetic chitosan nanoparticles for pH responsive targeted drug delivery. Eur. J. Pharm. Sci. 62, 243–250.
Unsoy, G., Yalcin, S., Khodadust, R., Mutlu, P., Onguru, O., Gunduz, U., 2014b. Chitosan magnetic nanoparticles for pH responsive Bortezomib release in cancer therapy. Biomed. Pharm. 68, 641–648.
Vandana, M., Sahoo, S.K., 2010. Long circulation and cytotoxicity of PEGylated gemcitabine and its potential for the treatment of pancreatic cancer. Biomaterials 31 (35), 9340–9356.
Wilczewska, A.Z., Niemirowicz, K., Markiewicz, K.H., Car, H., 2012. Nanoparticles as drug delivery systems. Pharmacol. Rep. 64 (5), 1020–1037.
Yongmei, X., Yumin, D., 2003. Effect of molecular structure of chitosan on protein delivery properties of chitosan nanoparticles. Int. J. Pharm. 250, 215–226.